

The contribution of age structure to cell population responses to targeted therapeutics

Pierre Gabriel^{*†} Shawn P. Garbett[‡] Darren R. Tyson[†] Glenn F. Webb[§]

December 8, 2011

Abstract

Cells grown in culture act as a model system for analyzing the effects of anticancer compounds, which may affect cell behavior in a cell cycle position-dependent manner. Cell synchronization techniques have been generally employed to minimize the variation in cell cycle position. However, synchronization techniques are cumbersome and imprecise and the agents used to synchronize the cells potentially have other unknown effects on the cells. An alternative approach is to determine the age structure in the population and account for the cell cycle positional effects post hoc. Here we provide a formalism to use quantifiable age distributions from live cell microscopy experiments to parameterize an age-structured model of cell population response.

Keywords: Cell cycle, intermitotic time, renewal equation, exponentially modified gaussian

1 Introduction

When examined individually in time lapse microscopy experiments, cells grown in culture display variability in the length of their cell cycles (between mitotic events), and this variability is represented by intermitotic time (IMT) distributions [20, 32, 33]. These distributions are usually obtained from asynchronously dividing populations of cells, which achieve a steady-state age structure when the population is growing exponentially. In experimental studies that examine the effects of perturbations on cellular proliferation, it is often desirable to determine whether the perturbation is affecting cells in particular stages within their cell cycle, i.e. whether the perturbation has cell cycle-specific effects. In this paper we provide a formalism to convert data obtained as IMT distributions to parameterize an age-structured population model and, thus, identifying the contribution of age structure to the response of the cell population to perturbation.

Models of age-structured populations using partial differential equations, such as those originally described by A. Lotka, A.G. McKendrick, W.O. Kermack, and F. von Foerster, are well adapted to

^{*}Université Pierre et Marie Curie-Paris 6, UMR 7598 LJLL, BC187, 4, place de Jussieu, F-75252 Paris cedex 5, France. Email: gabriel@ann.jussieu.fr

[†]Present address: INRIA Rhônes-Alpes, projet BEAGLE, Bâtiment CEI-1, BP 52132, 66 Boulevard Niels Bohr, F-69603 Villeurbanne cedex, France.

[‡]Department of Cancer Biology, Vanderbilt University, 2220 Pierce Ave., Nashville, TN 37232

[§]Department of Mathematics, Vanderbilt University, 1326 Stevenson Center, Nashville, TN 37240. Email: glenn.f.webb@vanderbilt.edu

model the dynamical features of experimental cultures of cells transiting the cell cycle with variable IMT. These models have been widely studied from a mathematical perspective [4, 3, 14, 15, 16, 21, 34, 36, 39, 45], but the application of the model to experimental data has been hampered by an inability to determine the age-dependent model parameters. The usual approach for parameter estimation is to solve numerically an inverse problem (see [1, 8, 9, 19, 18, 22, 26, 38, 40, 41, 42, 43, 37] on this question for structured population models), but this requires extensive input data and is specific to a given situation. A much more convenient approach is to assume that the distributed parameters lie in a class of functions with only a few constants (power laws or other forms [23]) and obtain the parameters from the fit of the functions to experimental data.

One function that often provides a better fit to IMT data than others, such as log-normal, inverse normal or gamma functions, is an exponentially modified Gaussian (EMG) [25, 44]. Under conditions in which the IMT distribution can be explained by an EMG model, we submit that the age-dependent division rate can be identified as an error function. Starting from this observation, we present a simple method to recover the parameters of this error function from parameters fitted to the experimental IMT data. Once reliably parameterized, the age-structured model can be used to make predictions about cell age-dependent effects of perturbations, for example, whether cells arrest during their cell cycle in response to treatment with antiproliferative compounds.

2 Intermittotic time and age-structured model

As with human populations, we can associate an age to each individual cell in a cell population. We define the age of a cell as the time elapsed from its last mitosis. Thus, the IMT of a cell is its age at division. This definition allows us to interpret the IMT distributions in terms of a dynamic age-structured population model.

Experimental IMT distributions can be seen as histograms which represent, for a given population, the density of cells with a certain age of division (see Figure 1 for an example taken from [44]). The age of division is distributed into N bins of width Δa . For all i between 1 and N , the height H_i of the i^{th} bar represents the density of cells with an age of division in the window $[i\Delta a, (i + 1)\Delta a]$. The histogram $(H_i)_{1 \leq i \leq N}$ is normalized to represent a density

$$\Delta a \sum_{i=1}^N H_i = 1. \quad (1)$$

We briefly explain here the method used in [44] to build IMT histograms (we refer to this paper for more details). The data are obtained using extended temporally resolved automated microscopy (ETRAM) in which cell nuclei are fluorescently labeled, imaged by automated time lapse fluorescence microscopy, and tracked as individual cells from the resultant image stacks. Cells are subjected to various microenvironmental conditions (such as the addition of a drug) at a specific time during image acquisition (set to time t_0) and the effect of the perturbation from that point in time is followed across the entire population and individual cells within it. The duration of observation (T) is chosen large enough to observe that almost all cycling cells divide before this final time. The data are organized into the bins to obtain a histogram, which is then normalized to represent a density of cells.

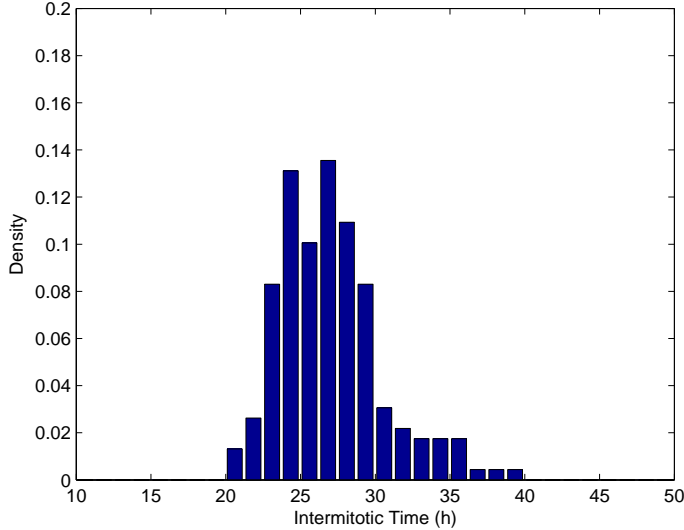


Figure 1: Plot of an histogram $(H_i)_{1 \leq i \leq N}$ representing the IMT distribution of a population of PC-9 lung cancer cells. The data is from [44] and the bin width is $\Delta a = \frac{10}{8}$.

The next step is to describe the IMT distributions in terms of an age-structured model and use this interpretation to parameterize the renewal equation, also known as the McKendrick–Von Foerster’s model, which is widely used to model the cell cycle. The partial differential equation for this model provides the evolution of the density $p(t, a)$ of cells with age a at time t

$$\begin{cases} \frac{\partial}{\partial t} p(t, a) + \frac{\partial}{\partial a} p(t, a) + \beta(a)p(t, a) = 0, & t \geq 0, \quad a > 0, \\ p(t, 0) = 2 \int_0^\infty \beta(a)p(t, a) da, \\ p(0, a) = p_0(a). \end{cases} \quad (2)$$

In this model, the cells age one-to-one with time at speed $\frac{da}{dt} = 1$, and divide with rate $\beta(a) \geq 0$. When a cell divides at mitosis, it produces two daughters with age $a = 0$, which is taken into account by the boundary condition at $a = 0$. The number of cells at time t with age between a_1 and a_2 is $\int_{a_1}^{a_2} p(t, a) da$, and the total number of cells at time t is $\int_0^\infty p(t, a) da$.

The division rate β has a probabilistic interpretation: the probability that a cell did not divide by age a is given by

$$\mathbb{P}(a) = e^{- \int_0^a \beta(a') da'}.$$

In this basic form of the model all cells are considered to be proliferating, and all must divide at some time (models including cell cycle arrest and death are described in subsequent sections). Thus, the division rate has to satisfy

$$\lim_{a \rightarrow +\infty} \int_0^a \beta(a') da' = +\infty. \quad (3)$$

Equation (2) is a transport equation which satisfies a maximum principle, namely if the initial distribution $p_0(a)$ is nonnegative (positive) then the distribution $p(t, a)$ remains nonnegative (positive)

for all time $t > 0$. The solutions of (2) have a remarkable behavior as time evolves, in that the age structure equilibrates no matter what the initial age structure of the population may be. This effect is known as *asynchronous exponential growth*, and its interpretation is that the population disperses over time to a limiting asymptotic equilibrium age structure where the fraction of the population in any age range $[a_1, a_2]$ satisfies

$$\lim_{t \rightarrow \infty} \frac{\int_{a_1}^{a_2} p(t, a) da}{\int_0^\infty p(t, a) da}$$

= a constant independent of the initial age structure [46]. Moreover, the solutions to this equation, as $t \rightarrow \infty$, are known to behave like a separated variables solution, that is, $p(t, a) = a$ function of time only \times a function of age only. More precisely, consider the eigenvalue problem

$$\begin{cases} \lambda \hat{p}(a) + \partial_a \hat{p}(a) + \beta(a) \hat{p}(a) = 0, \\ \hat{p}(0) = 2 \int_0^\infty \beta(a) \hat{p}(a) da, \\ \hat{p}(\cdot) > 0, \quad \int \hat{p}(a) da = 1, \end{cases} \quad (4)$$

This problem has a unique solution given by

$$\hat{p}(a) = \hat{p}(0) e^{-\int_0^a (\beta(a') + \lambda) da'}$$

where $\lambda > 0$ is the unique value such that

$$1 = 2 \int_0^\infty \beta(a) e^{-\int_0^a (\beta(a') + \lambda) da'} da \quad (5)$$

and

$$\hat{p}(0) = \left(\int_0^\infty e^{-\int_0^a (\beta(a') + \lambda) da'} da \right)^{-1}.$$

Then we can prove that, for large times,

$$p(t, a) \sim \text{const} \hat{p}(a) e^{\lambda t}$$

(see Appendix A for more details and references). If the population of cells proliferates over a sufficiently long time, we can assume that this asymptotic behavior is reached and use it to investigate the IMT distributions. An experimental observation that the total population (independent of age structure) is growing exponentially is an indicator that the population has effectively reached the equilibrium age distribution, which can be checked using ETRAM for other time series data collection (see Figure 2).

Now we give a continuous expression of the IMT distribution in terms of the age-structured model. The age distribution of the cells relative to time t_0 (time of perturbation) is given by a truncation of the equilibrium age distribution \hat{p}

$$\bar{p}_0(a) = \begin{cases} \rho e^{-\int_0^a (\beta(a') + \lambda) da'} & \text{if } 0 \leq a \leq t_0, \\ 0 & \text{if } a > t_0. \end{cases}$$

where ρ is a scaling constant. We then follow this age distribution along time and obtain for $t > 0$

$$\bar{p}(t, a) = \begin{cases} \rho e^{-\int_0^a (\beta(a') + \lambda) da'} e^{\lambda t} & \text{if } t \leq a \leq t + t_0, \\ 0 & \text{otherwise.} \end{cases}$$

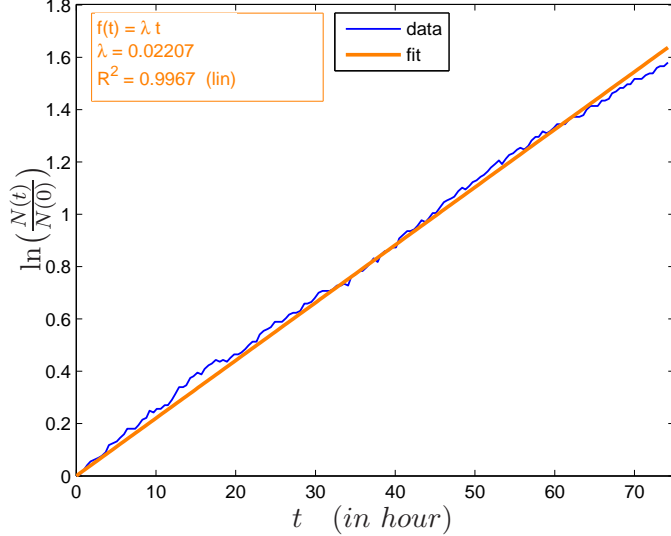


Figure 2: The evolution of the total population $N(t)$ is plotted on log-scale (blue) (the data is from [44]). The graph is well-fitted with a line of slope $\lambda = 0.022$ (correlation coefficient: $R^2 = 0.9967$). This gives evidences that the total population is growing exponentially fast with exponential constant λ . Thus, $N(t) = \exp^{\lambda t} N(0)$, and if t^* is the population doubling time, then $N(t^*) = 2N(0)$, and $t^* = \ln 2/\lambda$.

According to the age-structured model, and because of the normalization (1), the IMT distribution satisfies

$$I_T(a) := C_T^{-1} \int_0^T \beta(a) \bar{p}(t, a) dt, \quad C_T := \int_0^\infty \int_0^T \beta(a) \bar{p}(t, a) dt da, \quad (6)$$

by definition of the division rate β . The fact that no cell can divide in a time less than t_0 means

$$\forall a \leq t_0, \quad \beta(a) = 0. \quad (7)$$

Under this condition, for T large, the function I_T is close to the function

$$I_\infty(a) := \beta(a) e^{- \int_0^a \beta(a') da'}. \quad (8)$$

This convergence is made mathematically precise by the following claim (the proof is given in Appendix B for a more general case in which it is not assumed that $p(t, a)$ is close to the equilibrium age distribution):

Claim 1. *Under Assumptions (3) and (7), we have the convergence*

$$\int_0^\infty |I_T(a) - I_\infty(a)| da \xrightarrow{T \rightarrow \infty} 0.$$

Remark 2. *We can easily prove that, under the additional assumption*

$$\lim_{a \rightarrow +\infty} \beta(a) e^{- \int_0^a \beta(a') da'} = 0, \quad (9)$$

we also have

$$\sup_{a \geq 0} |I_T(a) - I_\infty(a)| \xrightarrow[T \rightarrow +\infty]{} 0.$$

Condition (9) is satisfied from Assumption (3), if for example, β bounded or monotonic.

Because in the experimental protocol T is chosen large enough to observe no dividing cells at the end, we can approximate I_T by I_∞ which has a simple expression in terms of the division rate (8).

3 From the intermitotic time to the division rate

The expression I_∞ can be inverted to recover the division rate from the IMT distribution (see [30, 13])

$$\beta(a) = \frac{I_\infty(a)}{\int_a^\infty I_\infty(a') da'}. \quad (10)$$

We start from the fitting of the experimental IMT distributions, which are observed to be positively skewed. From a fitting procedure for I_∞ , we use Equation (10) to recover the division rate of the renewal equation, which is very important for applications of age-structured models (see Section 5).

First consider as in [30] that the IMT distribution is a shifted gamma function (see also [12] and references therein). Setting

$$I_\infty(a|m, \sigma) = \begin{cases} 0 & \text{if } 0 \leq a \leq m, \\ \frac{a-m}{\sigma^2} e^{-\frac{a-m}{\sigma}} & \text{if } a \geq m, \end{cases} \quad (11)$$

we can solve explicitly Equation (10) and we find

$$\beta(a) = \begin{cases} 0 & \text{if } 0 \leq a \leq m, \\ \frac{a-m}{\sigma(\sigma+a-m)} & \text{if } a \geq m. \end{cases} \quad (12)$$

So by fitting an experimental IMT distribution with a shifted gamma function, we obtain two parameters m and σ which allows reconstruction of the division rate of the renewal equation.

To have a smoother transition at the minimum age of division m , one can consider a second shifted gamma function

$$I_\infty(a|m, \sigma) = \begin{cases} 0 & \text{if } 0 \leq a \leq m, \\ \frac{(a-m)^2}{2\sigma^3} e^{-\frac{a-m}{\sigma}} & \text{if } a \geq m. \end{cases} \quad (13)$$

Then the corresponding β is

$$\beta(a) = \begin{cases} 0 & \text{if } 0 \leq a \leq m, \\ \frac{1}{\sigma} \frac{(a-m)^2}{2\sigma^2 + 2\sigma(a-m) + (a-m)^2} & \text{if } a \geq m. \end{cases} \quad (14)$$

The different functions (11) to (14) are plotted in Figure 3

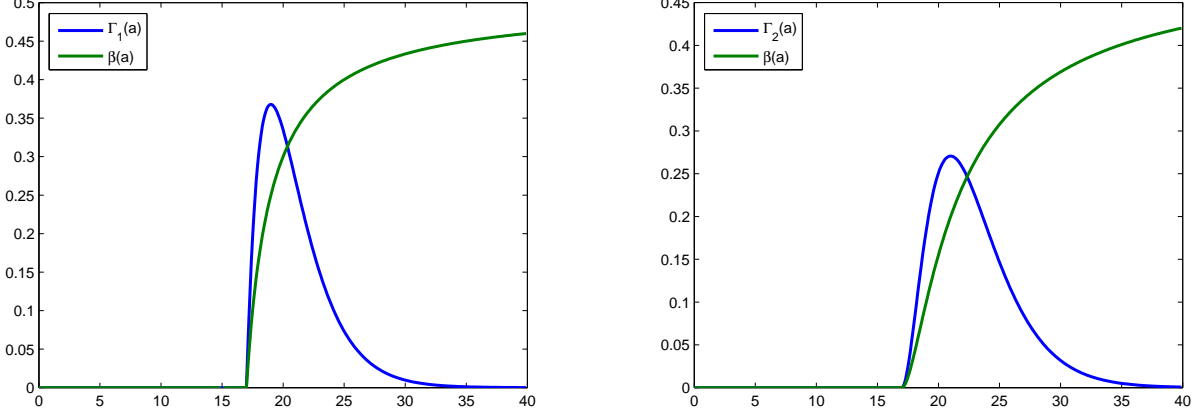


Figure 3: The two different gamma functions and their corresponding division rate $\beta(a)$ are plotted for coefficients $m = 17$ and $\sigma = 2$.

It has been observed that an exponentially modified Gaussian (EMG) is often a better model for IMT distributions than the gamma function [25, 44]. An EMG is defined as the convolution of a Gaussian with a decreasing exponential, but after solving it can be written with three parameters as

$$I_\infty(a|\beta_0, m, \sigma) = \beta_0 \operatorname{Erfc}\left(\frac{m-a}{\sigma}\right) e^{-2\beta_0\left(\frac{\beta_0\sigma^2}{2} - m + a\right)}. \quad (15)$$

where the (complementary) error function is defined by

$$\operatorname{Erfc}(z) = 1 - \frac{2}{\sqrt{\pi}} \int_0^z e^{-t^2} dt.$$

Replacing I_∞ by an EMG in Equation (10), we cannot compute explicitly the expression for β . But by numerical comparison, we obtain a division rate β that is essentially indistinguishable from an error function (see Figure 4).

Instead of fitting the IMT distribution by an EMG and then fitting the corresponding β by an error function, we may directly assume that β is an error function

$$\beta(a) = \beta_0 \operatorname{Erfc}\left(\frac{m-a}{\sigma}\right). \quad (16)$$

We can then explicitly derive a new fitting formula for I_∞ due to Equation (8)

$$I_\infty(a|\beta_0, m, \sigma) = \beta_0 \operatorname{Erfc}\left(\frac{m-a}{\sigma}\right) e^{-\int_0^a \beta_0 \operatorname{Erfc}\left(\frac{m-a'}{\sigma}\right) da'} \quad (17)$$

where the integral in the exponential can be computed as

$$\int_0^a \operatorname{Erfc}\left(\frac{m-a'}{\sigma}\right) da' = m \operatorname{Erfc}\left(\frac{m}{\sigma}\right) - \frac{\sigma}{\sqrt{\pi}} e^{-\left(\frac{m}{\sigma}\right)^2} - (m-a) \operatorname{Erfc}\left(\frac{m-a}{\sigma}\right) + \frac{\sigma}{\sqrt{\pi}} e^{-\left(\frac{m-a}{\sigma}\right)^2}. \quad (18)$$

Using this formula for the IMT instead of an EMG formula, the fitting parameters provide immediately the division rate β .

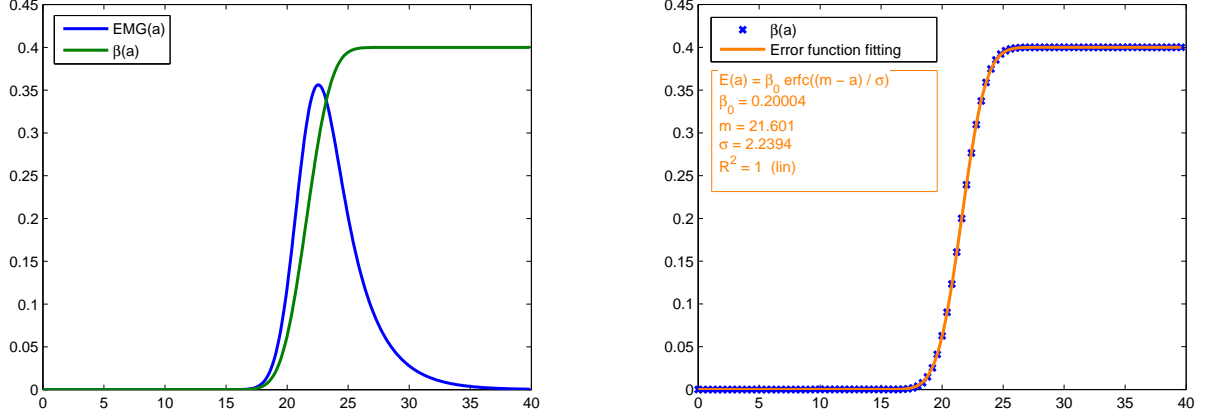


Figure 4: Left: The division rate $\beta(a)$ is obtained numerically from (10) by using an EMG with coefficients $m = 22$, $\sigma = 2$ and $\beta_0 = 0.2$ to fit I_∞ (15). Right: The formula for β , as an error function with these same three parameters, is numerically indistinguishable from the numerically obtained β ($R^2 = 1$).

When we know the Malthusian growth parameter (population growth rate λ) from experimental data (see Figure 2), it is possible to recover a division rate β such that relation (5) is satisfied. This is an important step in order to parameterize and apply an age-structured model to experimental data (see Section 5 below). We notice the relationship of β in terms of $I_\infty(a)$ is

$$2 \int_0^\infty I_\infty(a) e^{-\lambda a} da = 2 \int_0^\infty \beta(a) e^{-\int_0^a \beta(a') da'} e^{-\lambda a} da = 1.$$

To take advantage of this relationship between the IMT data, $\beta(a)$, and the malthusian parameter λ at the equilibrium distribution, we define a new histogram $(\tilde{H}_i)_{1 \leq i \leq N}$ by

$$\forall i, \quad \tilde{H}_i := \frac{2H_i e^{-\lambda a_i}}{\Delta a \sum_{i=1}^N 2H_i e^{-\lambda a_i}} \quad (19)$$

where $a_i := (i + \frac{1}{2})\Delta a$ is the mean age of the i^{th} bar. Thus defined, the new histogram incorporates information about λ and satisfies the relation

$$\Delta a \sum_{i=1}^\infty \tilde{H}_i = 1. \quad (20)$$

We then fit this new histogram (\tilde{H}_i) with the model

$$\tilde{I}_\infty(a) := 2I_\infty(a)e^{-\lambda a} \quad (21)$$

instead of fitting (H_i) with $I_\infty(a)$. Because of the normalization (20), we expect that the fitting provides parameters such that $\int_0^\infty \tilde{I}_\infty(a) da \approx 1$, and this relation can be checked numerically *a posteriori*.

Method and example. We divide the process in three steps and illustrate it by an example. Each required fitting step can be performed using the freely available Ezyfit Matlab toolbox [<http://www.fast.u-psud.fr/ezyfit/>].

Step 1: Determine equilibrium IMT distribution

- a) Obtain a histogram (H_i) for the experimental IMT distribution of control (untreated) cells. *Here we use an IMT distribution obtained in [44] for PC-9 lung cancer cells using ETRAM (see Figure 1).*
- b) Plot the time evolution of the total population on a \log_e -scale, verify a linear fit and obtain the slope as the experimental value for the Malthusian parameter λ of the cell population (see Figure 2 for an example).
- c) Construct the new histogram (\tilde{H}_i) from (H_i) and λ by using the definition (19).

Step 2: Obtain parameters from model fit to IMT distribution

- a) Choose a form for I_∞ as a gamma function (11) or (13), or as the new EMG form (17).
- b) Fit the histogram (\tilde{H}_i) with the corresponding form \tilde{I}_∞ from definition (21). *For PC-9 cancer cells we choose the form (17), because in [44] it was observed that the IMT distribution appeared to be an EMG (see Figure 5 for the example).*
- c) Verify that the correlation coefficient R^2 of the IMT data and the chosen form $\tilde{I}_\infty(a)$ is close to 1.

Step 3: Parameterize age-structured model

If numerical integral $\int_0^\infty \tilde{I}_\infty(a) da$ is close to 1, the fitting parameters provide a good approximation of the division rate β , which can then be propagated through the population, based on the choice of I_∞ . *In the example, β is given by Equation (16) with the numerical parameters of Figure 5.*

4 Model with a death rate

If it is known that the proliferating cells have a mortality rate $\mu(a) \geq 0$, then this mortality rate can be introduced in the renewal equation:

$$\begin{cases} \frac{\partial}{\partial t} p(t, a) + \frac{\partial}{\partial a} p(t, a) + \beta(a)p(t, a) + \mu(a)p(t, a) = 0, & t \geq 0, \quad a > 0, \\ p(t, 0) = 2 \int_0^\infty \beta(a)p(t, a) da, \\ p(0, a) = p_0(a). \end{cases} \quad (22)$$

We have the same result as before about the long-term behavior

$$p(t, a) \sim \text{const} \hat{p}(a) e^{\lambda t}$$

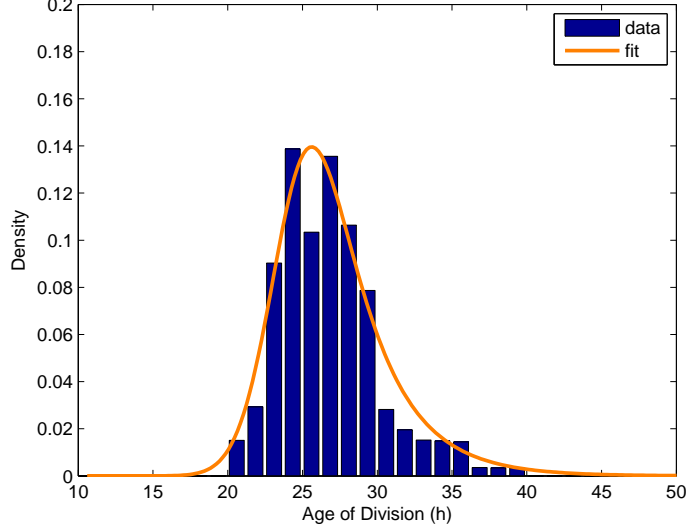


Figure 5: Fitting of experimental data in [44] with the model (17). The fitting parameters are $\beta_0 = 0.14204$, $m = 24.456$ and $\sigma = 3.3451$. The correlation coefficient is $R^2 = 0.95363$ and the integral of $\tilde{I}_\infty(a|\beta_0, m, \sigma)$ is $\int_0^\infty \tilde{I}_\infty(a) da \approx 1.0983$. The formula for the age dependent division rate is $\beta(a) = \beta_0 Ercf(\frac{m-a}{\sigma})$.

where the eigenfunction $\hat{p}(a)$ is now

$$\hat{p}(a) = \hat{p}(0) e^{-\int_0^a (\beta(a') + \mu(a') + \lambda) da'}$$

and the eigenvalue λ satisfies

$$2 \int_0^\infty \beta(a) e^{-\int_0^a (\beta(a') + \mu(a') + \lambda) da'} da' = 1. \quad (23)$$

Assuming that the stable distribution is reached, we define as in Section 2 the IMT function

$$I_T(a) := C_T^{-1} \int_0^T \beta(a) \bar{p}(t, a) dt$$

with

$$\bar{p}(t, a) = \rho e^{-\int_0^a (\beta(a') + \mu(a') + \lambda) da'} e^{\lambda t} \mathbb{1}_{t \leq a \leq t+T} \quad \text{and} \quad C_T = \int_0^\infty \int_0^T \beta(a) \bar{p}(t, a) dt da.$$

Adapting the proof of Theorem 3 in Appendix B, we obtain that $I_T(a)$ converges as $T \rightarrow \infty$ to

$$I_\infty(a) := C_\infty^{-1} \beta(a) e^{-\int_0^a (\beta(a') + \mu(a')) da'} \quad (24)$$

where

$$C_\infty := \int_0^\infty \beta(a) e^{-\int_0^a (\beta(a') + \mu(a')) da'} da. \quad (25)$$

For this model there does not exist an inversion formula as Equation (10) to recover β analytically. So we consider that β is a rational fraction given by Equation (12) or (14), or an error function given by

Equation (16), and we derive the corresponding model I_∞ from Equation (24). To use this model to fit IMT distributions, one has to prescribe the shape of the death rate. If we do not have any information about its age dependency, we assume that $\mu(a) \equiv \mu$ is age-independant, and thus an additional fitting parameter (a fixed rate based on measured data can also be used if available).

The constant C_∞ was equal to 1 in model (2), but if there is a positive death rate, we have that $C_\infty < 1$. This constant is a function of the fitting parameters (see Equation (25)), but we do not have an analytic expression of this function in general. A solution to this problem is to use the Malthusian parameter λ , which incorporates information about μ and $\beta(a)$, to define a form $\tilde{I}_\infty(a)$ as in Section 3. Indeed, because of relation (23), we obtain

$$\tilde{I}_\infty(a) := 2\beta(a)e^{-\int_0^a (\beta(a')+\mu) da'} e^{-\lambda a}$$

which does not involve C_∞ . Then, the division rate $\beta(a)$ is obtained from $\tilde{I}_\infty(a)$ as before using the modified histogram (\tilde{H}_i) defined from (H_i) by (19).

Example. We fit the same distribution as in Section 3 still considering that β is an error function. With a constant death rate μ , we obtain the four parameters model

$$\tilde{I}_\infty(a|\beta_0, m, \sigma, \mu) = 2\beta_0 \operatorname{Erfc}\left(\frac{m-a}{\sigma}\right) e^{-\int_0^a (\beta_0 \operatorname{Erfc}\left(\frac{m-a'}{\sigma}\right) + \mu + \lambda) da'} \quad (26)$$

where the integral $\int_0^a \beta_0 \operatorname{Erfc}\left(\frac{m-a'}{\sigma}\right) da'$ is given by Equation (18). The fitting provides new parameters for β and a positive death rate μ (see Figure 6). The correlation R^2 is slightly better than in Figure 5 and the integral $\int_0^\infty \tilde{I}_\infty(a) da$ is closer to 1. So we can consider that mortality has to be considered for this cell line.

5 Application

Once accurately parameterized, model (2) or (22) can be used for further investigations into the dynamics of age-structured cell populations. We give here one application for *in vitro* PC-9 cancer cell lines undergoing treatment by the drug erlotinib. It has been recently shown in [44] that the main effect of erlotinib on cancer cells is to induce entry into quiescence. In [44] a system of ordinary differential equations (without age structure) is used to model these experiments. We hypothesize here that erlotinib induced quiescence is linked to the age of the cells involved. Many age-structured models with quiescence can be found in the literature (see [7, 10, 11, 27, 28, 29] for examples). Here we present a simple age-structured model with quiescence which allows us to explain observed delays in response to erlotinib. We start from the observation that there is no effect of the treatment on total population growth during the first twenty hours (see Figure 7). This time corresponds almost exactly to the minimal age of division observed for PC-9 cells. It suggests that erlotinib acts only during a specific phase of the cell cycle, which based on its biological activity would be expected to be in G1. The model we present is based on this idea and considers a fractional rate f of cells that become quiescent in an age-dependent manner, where the fraction is assumed to reflect the dose of erlotinib used for the treatment. We estimate the value of f from data available in [44], and then compare numerical simulations of the model to the experimental data. Many numerical methods are available

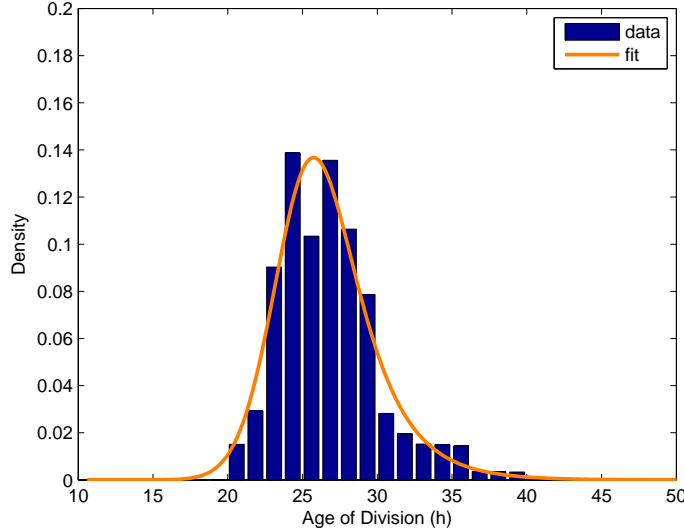


Figure 6: Fitting of experimental data with the model (26). The fitting parameters are $\beta_0 = 0.17879$, $m = 25.007$, $\sigma = 3.6141$ and $\mu = 0.00333$. The correlation coefficient is $R^2 = 0.95611$ and the integral of $\tilde{I}_\infty(a|\beta_0, m, \sigma)$ is $\int_0^\infty \tilde{I}_\infty(a) da \approx 1.0132$. The formula for the age dependent division rate is $\beta(a) = \beta_0 \text{Erfc}(\frac{m-a}{\sigma})$.

for structured population equations (see for instance [2, 6, 5, 17, 24, 31]). Here we use a scheme based on the method of characteristics, as in [6, 5, 31], for its anti-dissipative properties.

We start from the renewal equation (22) and we introduce the quantity $Q(t)$ of quiescent cells at time t . This quantity evolves according to an ordinary differential equation which is coupled to the renewal equation through the system

$$\left\{ \begin{array}{l} \frac{\partial}{\partial t} p(t, a) + \frac{\partial}{\partial a} p(t, a) + \beta(a)p(t, a) + \mu p(t, a) = 0, \quad t \geq 0, \quad a > 0, \\ p(t, 0) = 2(1-f) \int_0^\infty \beta(a)p(t, a) da, \\ p(0, a) = p_0(a), \\ \frac{d}{dt} Q(t) = 2f \int_0^\infty \beta(a)p(t, a) da - \nu Q(t), \\ Q(0) = Q_0. \end{array} \right. \quad (27)$$

The coefficient ν is the death rate of quiescent cells and $f \in [0, 1]$ represents the fraction of proliferating cells which become quiescent. The erlotinib treatment starts at time $t = 0$, so at this time there are no quiescent cells ($Q_0 = 0$). The age distribution of the proliferating cells is assumed to be at equilibrium as in Equation (22) (*i.e.* $p_0(a) = \text{const} \hat{p}(a)$). The experimental values of the total population $N(t)$ along time are plotted after normalization by the initial value $N(0)$ on a log-scale (see Figure 7). Because of this normalization, we consider an initial distribution such that $\int_0^\infty p_0(a) da = 1$ which leads to $p_0(a) = \hat{p}(a)$ because of the definition of \hat{p} .

The coefficients β and μ are parameterized from IMT distributions for cells without treatment using the model (26). To estimate the value of the fraction f for different doses of treatment, we use data available in [44]. The fraction F of quiescent cells is estimated by examination of whether cells treated with erlotinib divide or not before the end of the experiment. We want to use this experimental fraction F to estimate the coefficient f of the model. For the sake of simplicity, assume that the death rates μ and ν are 0 in (27). In this case, at the end of the labeling period t_0 , the quantity of labeled quiescent cells corresponds to $Q(t_0)$ and the quantity of proliferating cells corresponds to $\int_0^{t_0} p(t, 0) dt$. Thus, the fraction F of quiescent cells at t_0 is

$$F = \frac{Q(t_0)}{Q(t_0) + \int_0^{t_0} p(t, 0) dt}. \quad (28)$$

Now we compute this quantity from model (27), keeping in mind that we have assumed no mortality. We have

$$\begin{aligned} Q(t_0) &= \int_0^{t_0} \frac{dQ}{dt}(t) dt \\ &= 2f \int_0^{t_0} \int_0^\infty \beta(a) p(t, a) da dt \end{aligned}$$

and

$$\int_0^{t_0} p(t, 0) dt = 2(1 - f) \int_0^{t_0} \int_0^\infty \beta(a) p(t, a) da dt.$$

Finally we obtain

$$\frac{Q(t_0)}{Q(t_0) + \int_0^{t_0} p(t, 0) dt} = \frac{2f}{2f + 2(1 - f)} = f.$$

So when there is no death rate, the experimental fraction F corresponds exactly to the coefficient f . In our simulations we consider positive death rates as suggested in Section 4. Since we cannot directly measure the coefficient ν , we assume that its value is close to the value of μ . Because the numerical values of ν and μ are similar and very small ($\mu \ll 1$), we can consider that f is still well-approximated by F and we use the fractions found in [44] to parameterize f . We can see in Figure 7 that the numerical simulations are very similar to the experimental curves. In particular, the delay of twenty hours before the effect of the treatment on the growth of the population is apparent, and this twenty hour period pulses two more times as the population approaches a new equilibrium distribution during the total time of the experiment. We have thus developed an age-structured model that can explain the dynamic effects of erlotinib on PC-9 cells, which are intrinsically dependent on the age of proliferating cells.

Conclusion

Linking experimental observation of cell behavior between the single-cell and population scales has recently been described using newly developed mathematical models [44]. However, this approach does not take into account the possible cell age-dependent effects of a perturbation on cell behavior, such as would be expected if the effects occur in cells at a specific position in the cell cycle. Since

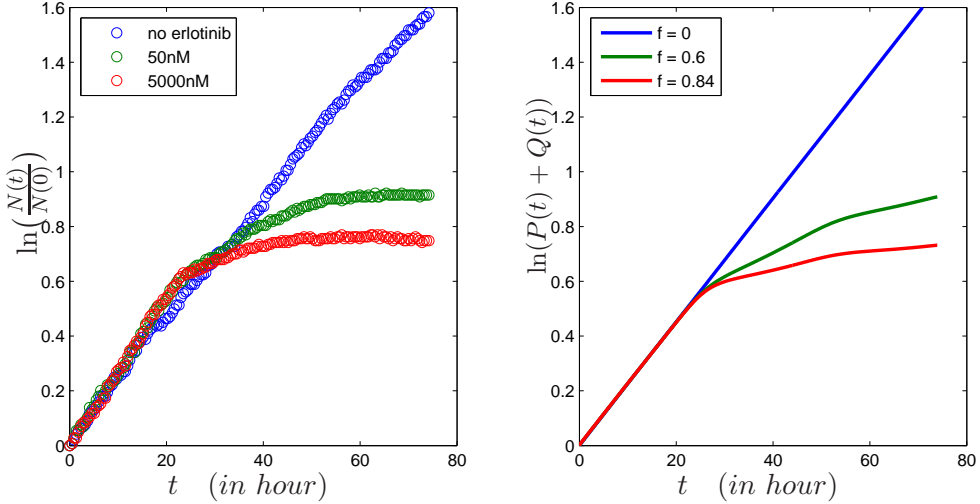


Figure 7: Left: experimental data without erlotinib, with a $50nM$ dose and with a $5000nM$ dose. The total quantity $N(t)$ is plotted on a log-scale. Right: numerical simulation of model (27) for $f = 0$, $f = 0.6$ and $f = 0.84$. The curves represent the evolution of $\ln(P(t) + Q(t))$ where $P(t) := \int_0^\infty p(t, a) da$ is the total quantity of proliferating cells at time t . They are obtained by solving numerically Equation (27) with the parameters of Figure 6 and with $\nu = 0.004$.

these studies were performed with asynchronously dividing cell populations, it is evident that the mathematical models of these experiments should have age structure as a primary feature. In fact, to fit the data, the authors had to use an artificial time offset to account for the age-structured effects. Here we provide a formalized approach to accurately account for cell age-dependent effects on cellular behavior. A major difficulty in the parameterization of age-structured models is the determination of the age dependent division rate. Our study provides a method for the quantitative recovery of this rate by fitting experimental IMT distributions to special forms, such as gamma functions or exponential modified Gaussians. This model, once successfully parameterized, is very useful for simulating and analyzing age-dependent phenomena in cell population dynamics. We have presented one such application for the *in vitro* treatment of cancer cells by erlotinib. This example shows the utility of age-structured population models in explaining the connection of drug therapy to phenomena such as cell cycle phase entry into quiescence. The method we have presented can be implemented readily to many issues in cell population behavior when there is experimental data based on cell age.

Acknowledgments

The research stays of P. Gabriel at Vanderbilt University have been financially supported by a grant of the *Fondation Pierre Ledoux Jeunesse Internationale*.

A Convergence to the equilibrium

The long-time behavior $p(t, a) \sim \text{const } \hat{p}(a) e^{\lambda t}$ can be proven by using semi-groups methods (see [34, 45]) or General Relative Entropy (see [35, 36]) techniques. We detail here a result provided by General Relative Entropy.

Consider ϕ the unique solution to the adjoint eigenvalue problem

$$\begin{cases} \lambda\phi(a) - \partial_a\phi(a) + \beta(a)\phi(a) = 2\phi(0)\beta(a), \\ \phi(\cdot) \geq 0, \quad \int \hat{p}(a)\phi(a) da = 1. \end{cases}$$

Then the General Relative Entropy method (see [35, 36]) allows us to prove that

$$\int_0^\infty |p(t, a)e^{-\lambda t} - \rho_0 \hat{p}(a)|\phi(a) da \xrightarrow[t \rightarrow \infty]{} 0$$

where

$$\rho_0 = \int_0^\infty \phi(a)p_0(a) da.$$

B Convergence of the IMT distribution

Theorem 3. *Suppose that Assumptions (3) and (7) are satisfied and consider an initial distribution \bar{p}_0 such that $\bar{p}_0(a) = 0$ for all $a > t_0$. Then we have the convergence*

$$\int_0^\infty |I_T(a) - I_\infty(a)| da \xrightarrow[T \rightarrow \infty]{} 0$$

where I_T and I_∞ are defined in (6) and (8).

Proof. First we extend the initial distribution and the division rate $\beta(a)$ to negative ages by setting $\bar{p}_0(a) = \beta(a) = 0$ for $a < 0$. Since the daughters of the labeled cells are not tracked, the age distribution $\bar{p}(t, a)$ of labeled cells satisfies a transport equation without boundary condition. Thus it writes, using the characteristic method,

$$\forall t, a \geq 0, \quad \bar{p}(t, a) = \bar{p}_0(a - t) e^{-\int_0^t \beta(a-s) ds}.$$

Introducing this expression in the definition of $I_T(a)$ we obtain, with changes of variables,

$$\begin{aligned} I_T(a) &= C_T^{-1} \int_0^T \beta(a)\bar{p}_0(a-t) e^{-\int_0^t \beta(a-s) ds} dt \\ &= C_T^{-1} \int_0^T \beta(a)\bar{p}_0(a-t) e^{-\int_{a-t}^a \beta(a') da'} dt \\ &= C_T^{-1} \int_{a-T}^a \beta(a)\bar{p}_0(u) e^{-\int_u^a \beta(a') da'} du \\ &= C_T^{-1} \beta(a) e^{-\int_0^a \beta(a') da'} \int_{a-T}^a \bar{p}_0(u) e^{\int_0^u \beta(a') da'} du. \end{aligned}$$

Since the support of \bar{p}_0 is included in $[0, t_0]$ and $\beta(a) = 0$ for $a \in [0, t_0]$ due to Assumption (3), we have for all $u \in \mathbb{R}$

$$\bar{p}_0(u) e^{\int_0^u \beta(a') da'} = \bar{p}_0(u)$$

so $I_T(a)$ writes

$$I_T(a) = C_T^{-1} \beta(a) e^{-\int_0^a \beta(a') da'} \int_{a-T}^a \bar{p}_0(u) du.$$

Define the primitive

$$P(a) := \int_0^a \bar{p}_0(u) du.$$

This function is nondecreasing and satisfies $P(a) = 0$ for $a \leq 0$ and $P(a) = P(t_0) = \int_0^\infty \bar{p}_0$ for $a \geq t_0$, so we have

$$\int_{a-T}^a \bar{p}_0(u) du = P(a) - P(a-T) = \begin{cases} P(a) & \text{if } 0 \leq a \leq t_0, \\ P(t_0) & \text{if } t_0 \leq a \leq T, \\ P(t_0) - P(a-T) & \text{if } T \leq a \leq T+t_0, \\ 0 & \text{if } a \geq T+t_0. \end{cases}$$

Because $\beta(a) = 0$ for $a \leq t_0$, we obtain by integration of $I_T(a)$ on \mathbb{R}^+

$$1 = C_T^{-1} P(t_0) \int_0^T \beta(a) e^{-\int_0^a \beta(a') da'} da + C_T^{-1} \int_T^{T+t_0} \beta(a) e^{-\int_0^a \beta(a') da'} (P(t_0) - P(a-T)) da$$

which gives

$$\begin{aligned} C_T - P(t_0) \int_0^T \beta(a) e^{-\int_0^a \beta(a') da'} da &= \int_T^{T+t_0} \beta(a) e^{-\int_0^a \beta(a') da'} (P(t_0) - P(a-T)) da \\ &\leq P(t_0) \int_T^{T+t_0} \beta(a) e^{-\int_0^a \beta(a') da'} da \\ &\xrightarrow[T \rightarrow +\infty]{} 0. \end{aligned}$$

Since

$$\int_0^\infty \beta(a) e^{-\int_0^a \beta(a') da'} da = 1,$$

we conclude that

$$C_T \xrightarrow[T \rightarrow +\infty]{} P(t_0) = \int_0^\infty \bar{p}_0(a) da.$$

Then we have

$$\begin{aligned} \int_0^\infty |I_T(a) - I_\infty(a)| da &\leq |C_T^{-1} P(t_0) - 1| \int_0^T \beta(a) e^{-\int_0^a \beta(a') da'} da \\ &\quad + \int_T^{T+t_0} |C_T^{-1} [P(t_0) - P(a-T)] - 1| \beta(a) e^{-\int_0^a \beta(a') da'} da \\ &\quad + \int_{T+t_0}^\infty \beta(a) e^{-\int_0^a \beta(a') da'} da \\ &\leq |C_T^{-1} P(t_0) - 1| \int_0^T \beta(a) e^{-\int_0^a \beta(a') da'} da + K \int_T^\infty \beta(a) e^{-\int_0^a \beta(a') da'} da \\ &\xrightarrow[T \rightarrow \infty]{} 0 \end{aligned}$$

and it ends the proof of Theorem 3. □

References

- [1] A. S. Ackleh. Parameter identification in size-structured population models with nonlinear individual rates. *Math. Comp. Modelling*, 30(9-10):81 – 92, 1999.
- [2] A. S. Ackleh and K. Ito. An implicit finite difference scheme for the nonlinear size-structured population model. *Numer. Funct. Anal. Optim.*, 18(9-10):865–884, 1997.
- [3] B. Ainseba and C. Benosman. Cml dynamics: Optimal control of age-structured stem cell population. *Math. Comput. Simul.*, 81(10):1962–1977, 2011.
- [4] B. Ainseba, D. Picart, and D. Thiéry. An innovative multistage, physiologically structured, population model to understand the european grapevine moth dynamics. *J. Math. Anal. Appl.*, 382(1):34–46, 2011.
- [5] O. Angulo and J. López-Marcos. Numerical integration of fully nonlinear size-structured population models. *Appl. Num. Math.*, 50(3-4):291 – 327, 2004.
- [6] O. Angulo and J. C. López-Marcos. Numerical integration of nonlinear size-structured population equations. *Ecol. Modelling*, 133(1-2):3–14, 2000.
- [7] O. Arino, E. Sánchez, and G. F. Webb. Necessary and sufficient conditions for asynchronous exponential growth in age structured cell populations with quiescence. *J. Math. Anal. Appl.*, 215(2):499–513, 1997.
- [8] H. T. Banks, J. E. Banks, L. K. Dick, and J. D. Stark. Estimation of dynamic rate parameters in insect populations undergoing sublethal exposure to pesticides. *Bull. Math. Biol.*, 69:2139–2180, 2007.
- [9] H. T. Banks, K. L. Sutton, W. C. Thompson, G. Bocharov, M. Doumic, T. Schenkel, J. Araguilaguet, S. Giest, C. Peligero, and A. Meyerhans. A new model for the estimation of cell proliferation dynamics using cfse data. *J. of Immunological Methods*, To appear, 2011.
- [10] F. Bekkal Brikci, J. Clairambault, and B. Perthame. Analysis of a molecular structured population model with possible polynomial growth for the cell division cycle. *Math. Comput. Modelling*, 47(7-8):699–713, 2008.
- [11] F. Bekkal Brikci, J. Clairambault, B. Ribba, and B. Perthame. An age-and-cyclin-structured cell population model for healthy and tumoral tissues. *J. Math. Biol.*, 57(1):91–110, 2008.
- [12] S. Bernard, L. Pujo-Menjouet, and M. C. Mackey. Analysis of cell kinetics using a cell division marker: Mathematical modeling of experimental data. *Biophys J.*, 84(5):3414–3424, May 2003.
- [13] F. Billy, J. Clairambault, O. Fercoq, S. Gaubert, T. Lepoutre, T. Ouillon, and S. Saito. Synchronisation and control of proliferation in cycling cell population models with age structure. *Math. Comp. Simul.*, Accepted, 2011.
- [14] A. Calsina and J. Saldaña. A model of physiologically structured population dynamics with a nonlinear individual growth rate. *J. Math. Biol.*, 33:335–364, 1995.
- [15] P. Clément, H. J. A. M. Heijmans, S. Angenent, C. J. van Duijn, and B. de Pagter. *One-parameter semigroups*, volume 5 of *CWI Monographs*. North-Holland Publishing Co., Amsterdam, 1987.

- [16] O. Diekmann, H. J. A. M. Heijmans, and H. R. Thieme. On the stability of the cell size distribution. *J. Math. Biol.*, 19:227–248, 1984.
- [17] J. Douglas and F. Milner. Numerical methods for a model of population dynamics. *Calcolo*, 24:247–254, 1987.
- [18] M. Doumic, P. Maia, and J. Zubelli. On the calibration of a size-structured population model from experimental data. *Acta Biotheoretica*, 58:405–413, 2010.
- [19] M. Doumic, B. Perthame, and J. Zubelli. Numerical solution of an inverse problem in size-structured population dynamics. *Inverse Problems*, 25(4):045008, 2009.
- [20] M. R. Dowling, D. Milutinovi, and P. D. Hodgkin. Modelling cell lifespan and proliferation: is likelihood to die or to divide independent of age? *Journal of The Royal Society Interface*, 2(5):517–526, 2005.
- [21] K.-J. Engel and R. Nagel. *One-parameter semigroups for linear evolution equations*, volume 194 of *Graduate Texts in Mathematics*. Springer-Verlag, New York, 2000. With contributions by S. Brendle, M. Campiti, T. Hahn, G. Metafune, G. Nickel, D. Pallara, C. Perazzoli, A. Rhandi, S. Romanelli and R. Schnaubelt.
- [22] H. Engl, W. Rundell, and O. Scherzer. A regularization scheme for an inverse problem in age-structured populations. *J. Math. Anal. Appl.*, 182(3):658 – 679, 1994.
- [23] P. Gabriel. The shape of the polymerization rate in the prion equation. *Math. Comput. Modelling*, 53(7-8):1451–1456, 2011.
- [24] P. Gabriel and L. M. Tine. High-order WENO scheme for polymerization-type equations. *ESAIM Proc.*, 30:54–70, 2010.
- [25] A. Golubev. Exponentially modified Gaussian (EMG) relevance to distributions related to cell proliferation and differentiation. *J. Theor. Biol.*, 262(2):257–266, 2010.
- [26] M. Gyllenberg, A. Osipov, and L. Päivärinta. The inverse problem of linear age-structured population dynamics. *J. Evol. Equ.*, 2(2):223–239, 2002.
- [27] M. Gyllenberg and G. F. Webb. Age-size structure in populations with quiescence. *Math. Biosci.*, 86(1):67–95, 1987.
- [28] M. Gyllenberg and G. F. Webb. A nonlinear structured population model of tumor growth with quiescence. *J. Math. Biol.*, 28(6):671–694, 1990.
- [29] M. Gyllenberg and G. F. Webb. Quiescence in structured population dynamics: applications to tumor growth. In *Math. pop. dyn. (New Brunswick, NJ, 1989)*, volume 131 of *Lecture Notes in Pure and Appl. Math.*, pages 45–62. Dekker, New York, 1991.
- [30] P. Hinow, S. Wang, C. Arteaga, and G. Webb. A mathematical model separates quantitatively the cytostatic and cytotoxic effects of a HER2 tyrosine kinase inhibitor. *Theo. Biol. Med. Modelling*, 4(1):14, 2007.
- [31] T. Kostova. An explicit third-order numerical method for size-structured population equations. *Numer. Methods Partial Diff. Equ.*, 19(1):1–21, 2003.

- [32] H. Lee and A. Perelson. Modeling t cell proliferation and death in vitro based on labeling data: Generalizations of the smithmartin cell cycle model. *Bull. Math. Biol.*, 70:21–44, 2008.
- [33] D. Liu, D. M. Umbach, S. D. Peddada, L. Li, P. W. Crockett, and C. R. Weinberg. A random-periods model for expression of cell-cycle genes. *Proceedings of the National Academy of Sciences of the United States of America*, 101(19):7240–7245, 2004.
- [34] J. A. J. Metz and O. Diekmann, editors. *The dynamics of physiologically structured populations*, volume 68 of *Lecture Notes in Biomathematics*. Springer-Verlag, Berlin, 1986. Papers from the colloquium held in Amsterdam, 1983.
- [35] P. Michel, S. Mischler, and B. Perthame. General relative entropy inequality: an illustration on growth models. *J. Math. Pures Appl.*, 84(9):1235–1260, 2005.
- [36] B. Perthame. *Transport equations in biology*. Frontiers in Mathematics. Birkhäuser Verlag, Basel, 2007.
- [37] B. Perthame and J. Zubelli. On the inverse problem for a size-structured population model. *Inverse Problems*, 23(3):1037–1052, 2007.
- [38] D. Picart and B. Ainseba. Parameter identification in multistage population dynamics model. *Nonlin. Anal.: Real World Appl.*, 12(6):3315 – 3328, 2011.
- [39] D. Picart, B. Ainseba, and F. Milner. Optimal control problem on insect pest populations. *Appl. Math. Lett.*, 24(7):1160–1164, 2011.
- [40] M. Pilant and W. Rundell. Determining a coefficient in a first-order hyperbolic equation. *SIAM J. Appl. Math.*, 51(2):pp. 494–506, 1991.
- [41] M. Pilant and W. Rundell. Determining the initial age distribution for an age structured population. *Math. Pop. Studies*, 3(1):3–20, 1991.
- [42] W. Rundell. Determining the birth function for an age structured population. *Math. Pop. Studies*, 1(4):377–395, 1989.
- [43] W. Rundell. Determining the death rate for an age-structured population from census data. *SIAM J. Appl. Math.*, 53(6):pp. 1731–1746, 1993.
- [44] D. R. Tyson, S. P. Garbett, P. L. Frick, and V. Quaranta. A method to quantify population-level cell proliferation dynamics from single-cell data. submitted.
- [45] G. F. Webb. *Theory of nonlinear age-dependent population dynamics*, volume 89 of *Monographs and Textbooks in Pure and Applied Mathematics*. Marcel Dekker Inc., New York, 1985.
- [46] G. F. Webb. An operator-theoretic formulation of asynchronous exponential growth. *Trans. Amer. Math. Soc.*, 303(2):751–763, 1987.